Applied Surface Science 256 (2010) 2110–2114

Contents lists available at ScienceDirect

Applied Surface Science

journal homepage: www.elsevier.com/locate/apsusc

Electrochemical synthesis of Cu/ZnO nanocomposite films and their efficient field emission behaviour

Farid Jamali Sheini [a,1], Jai Singh [b], O.N. Srivasatva [b], Dilip S. Joag [c], Mahendra A. More [c,*]

[a] Islamic Azad University, Ahwaz Branch, Ahwaz, Iran
[b] Center for Advanced Studies, Department of Physics, Banaras Hindu University, Varanasi 221005, India
[c] Center for Advanced Studies in Materials Science and Condensed Matter Physics, Department of Physics, University of Pune, Pune 411007, India

ARTICLE INFO

Article history:
Received 7 September 2009
Received in revised form 15 September 2009
Accepted 15 September 2009
Available online 24 September 2009

Keywords:
Cu nanoparticles
ZnO
Electrodeposition
Fowler–Nordheim plot

ABSTRACT

The Cu/ZnO nanocomposite films have been synthesized by cathodic electrodeposition and characterized using X-ray diffractometer (XRD), scanning electron microscope (SEM), transmission electron microscope (TEM), photoluminescence (PL) and field emission microscope (FEM). The XRD pattern shows a set of well defined diffraction peaks, which could be indexed to the wurtzite hexagonal phase of ZnO. In addition, characteristic diffraction peaks corresponding to Cu and Zn are also observed. The SEM image shows formation of two-dimensional (2D) hexagonal sheets randomly distributed and aligned almost normal to the substrate. Uniformly distributed small clusters of Cu nanoparticles possessing average diameter of ~25 nm, as revealed from the TEM image, are seen to be present on these 2D ZnO sheets. The selected area electron diffraction (SAED) image confirms the nanocrystalline nature of the Cu particles. From the field emission studies, carried out at the base pressure of $\sim 1 \times 10^{-8}$ mbar, the turn-on field required for an emission current density of 0.1 μA/cm^2 is found to be 1.56 V/μm and emission current density of ~100 μA/cm^2 has been drawn at an applied field of 3.12 V/μm. The Cu/ZnO nanocomposite film exhibits good emission current stability at the pre-set value of ~10 μA over a duration of 5 h. The simplicity of the synthesis route coupled with the better emission properties propose the electrochemically synthesized Cu/ZnO nanocomposite film emitter as a promising electron source for high current density applications.

1. Introduction

Improvement in the field emission properties of semiconductors can be achieved either by tailoring the geometry of the emitter or by modifying the electronic properties. However, the first approach has limitation in synthesizing anisotropic nanostructures possessing very fine apex radius, typically less than 10 nm. Similarly preparation of the emitters with modified electronic properties by doping/mixing with suitable elements is not easy, as the chemical reactivity may deteriorate their emission performance. Therefore, a proper combination of the two approaches is considered to be a viable alternative to achieve better field emission performance and has been effectively used by various researchers. The early results in this regard are due to Jo et al. who have reported ultra-low threshold field of 0.7 V/μm (corresponding to 1 mA/cm^2 current density) for ZnO nanowires deposited on the carbon cloth [1]. Attempt has been made to improve the field emission properties of ZnO nanowires by coating them with amorphous carbon and carbon nitride films [2]. Enhanced band gap emission has been observed in case of ZnO nanorods coated with Pt nanoparticles [3]. Following this, Ye et al. have observed enhanced field emission performance of ZnO nanorods by decorating them with Pt and Ag nanoparticles [4]. Very recently we have investigated field emission characteristics of ZnO nanoneedles coated on chemical vapour deposited diamond films and have observed improvement in the emission performance [5].

Amongst the numerous synthesis routes employed to grow ZnO nanostructures, electrochemical synthesis has been recognized as a potential technique because it is simple, economic and easy to scale up to industrial level. Moreover, it facilitates *in situ* doping and/or decorating of the nanostructures. We have effectively used this characteristic and synthesized Cu/ZnO nanocomposite films on zinc substrate.

In this paper we report on the synthesis of Cu/ZnO nanocomposite films, and their field emission studies. The value of the turn-on field, required to draw an emission current density of 0.1 μA/cm^2, was found to be 1.56 V/μm, which is found to be

* Corresponding author. Tel.: +91 20 25692678; fax: +91 20 25691684.
E-mail address: mam@physics.unipune.ernet.in (M.A. More).
[1] Present address: Department of Physics, University of Pune, Pune 411007, India.

0169-4332/$ – see front matter © 2009 Elsevier B.V. All rights reserved.
doi:10.1016/j.apsusc.2009.09.056

lower than those reported in the literature for various nanostructures [6–16]. In passing, it may be pointed out that most of the studies on field emission from ZnO nanostructures so far have been made on nanorods/nanoneedles. Only sparse studies have been carried out on nano-films/nanosheets.

2. Experimental

The synthesis of Cu/ZnO films was performed in a conventional three-electrode electrochemical cell. An aqueous solution containing a mixture of $ZnCl_2$, $CuCl_2$ and H_2O_2 (analytical grade) of concentrations ~16×10^{-3} M, 16×10^{-3} M and 4×10^{-3} M, respectively, was used as an electrolyte. All the deposition experiments were carried out at 82 °C, in which a polycrystalline Zn foil (99.99% pure, Alfa Aesar), a platinum sheet and a saturated calomel electrode (SCE, E_0 = 0.244 V vs. NHE) served as the working, counter and reference electrodes, respectively. Prior to the deposition, the Zn foil (substrate) and platinum electrode were ultrasonically cleaned in acetone and methanol successively for 10 min. A computer controlled electrochemical analyzer (Model-1100A Series, CH Instrument, USA) was used to maintain the cathodic polarization condition at −1.4 V with respect to the SCE. The electrolyte was constantly stirred during the synthesis and after a fixed deposition time (20 min) the working electrode was removed from the electrolyte, washed in gentle flow of water, and dried in air. At least four specimens were synthesized under identical experimental conditions and characterized by various analytical techniques in order to check the reproducibility and repeatability of the results.

The as-synthesized films were characterized by X-ray diffractometer (XRD) (D8, Advance, Bruker AXS model) with Cu Kα (λ: 1.5406 nm) as the incident radiation. The scanning electron microscope (SEM) observations were carried out with the operating voltage of 20 kV and the emission current ~60 μA (model JEOL, JSM-6360A). The elemental composition was obtained using energy-dispersive X-ray spectrometer (EDS) attached to the SEM instrument with the operating voltage of 20 kV, collection time was 80 s and the number of spots analyzed was 4 (~25 μm^2 area each). For the transmission electron microscope (TEM) analysis (model Philips, EM-CM-12) the specimens were prepared by scraping the Cu/ZnO film from the substrates. The scraped material was dispersed and sonicated in acetone. A small quantity of this solution was dropped on the TEM grid. The optical properties were investigated from the photoluminescence (PL) spectra recorded at room temperature using a Xenon lamp as the source (Photoluminescence Spectrometer, PerkinElmer-LS-55). The exciting wavelength was ~325 nm. The field emission current versus applied voltage (I–V) and current versus time (I–t) characteristics were recorded in a planar diode configuration in a vacuum chamber evacuated to a base pressure of ~1.0×10^{-8} mbar. The Cu/ZnO film synthesized on Zn foil served as an emitter cathode. A semi-transparent phosphor screen, used as an anode, was held parallel to the cathode at a distance of ~1 mm. The details of the field emission system and vacuum processing of the chamber are reported elsewhere [17]. The emission current data was acquired using auto ranging a Keithley 485 picoammeter, by varying the applied DC voltage between the cathode and the anode in steps of 40 V (0–40 kV, Spellman, USA). Care was taken to avoid any leakage current by ensuring proper grounding. At least two specimens, synthesized under identical experimental conditions, were subjected to the field emission studies so as to check the reproducibility of the results.

3. Results and discussion

The various chemical reactions occurring in the aqueous electrolyte resulting in cathodic electrodeposition of Cu/ZnO composite films are as given below:

$$H_2O_2 + 2e^- \rightarrow 2OH^- \quad (1)$$

$$O_2 + 2H_2O + 4e^- \rightarrow 4OH^- \quad (2)$$

$$Cu^{2+} + 2e^- \rightarrow Cu \quad (3)$$

$$Zn^{2+} + 2OH^- \rightarrow ZnO + H_2O \quad (4)$$

The hydroxide ions produced by reduction of H_2O_2 and water decomposition, reactions (1) and (2), usually increase local pH at the cathode. Cu^{2+} ions are reduced to Cu metal particles as per reaction (3). The Cu metal particles agglomerate to form larger particles. The Zn^{2+} ions in the solution form $Zn(OH)_2$ at the cathode which subsequently dehydrates into ZnO, according to reaction (4). The reduction potential of Cu^{2+} ions and Zn^{2+} ions are 0.3916 V and −0.7618 V, respectively (with reference to the saturated hydrogen electrode), which indicate that the possibility of oxidation of Cu^{2+} ions is less favourable than that of Zn^{2+} ions in the vicinity of the cathode. Therefore it could expected that formation of the Cu_2O or CuO phases during electrochemical synthesis is thermodynamically likely to be forbidden.

A typical XRD pattern of the as-synthesized Cu/ZnO film is shown in Fig. 1. The XRD pattern shows a set of well defined diffraction peaks, majority of the peaks could be indexed to the wurtzite hexagonal phase of ZnO. In addition diffraction peaks corresponding to Cu and Zn are also observed. The appearance of the diffraction peak corresponding to Zn is due to the fact that Zn has been used as a substrate in the present study. It is interesting to note that no diffraction peaks corresponding to phases of copper oxide are observed. The average crystal size of the Cu particles, obtained using the Debye–Scherer formula, is estimated to be ~26 nm. Thus, the XRD pattern clearly reveals formation of ZnO along with Cu crystallites in the synthesized film. The average thickness of the Cu/ZnO film, measured using Taly step method is found to be ~80 μm.

The surface morphology of the Cu/ZnO composite film as revealed from the SEM image (Fig. 2(a) and its inset) is characterized by two distinct features, randomly distributed two-dimensional ZnO sheets and small clusters/agglomerates of Cu particles. Formation of similar 2D hexagonal sheets of ZnO has been observed during electrochemical synthesis of ZnO [18]. The hexagonal ZnO sheets are seen to be aligned almost normal to the Zn substrate with average thickness of ~0.5 μm. Fig. 2(b) shows the TEM image of the Cu/ZnO composite film revealing nanometric dimensions of the copper particles present on the surface of the ZnO microsheets. The average diameter of the copper nanoparticles is found to be ~25 nm, which is consistent with the XRD

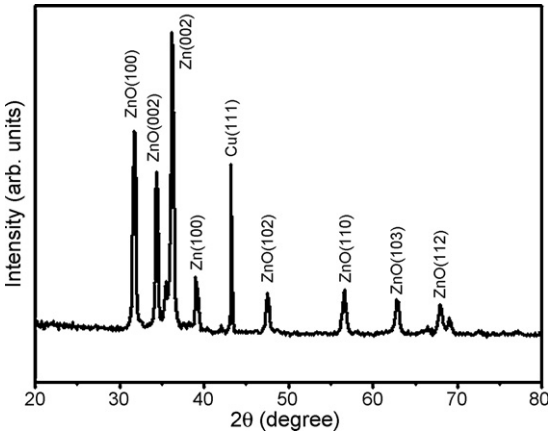

Fig. 1. XRD pattern of Cu/ZnO nanocomposite film.

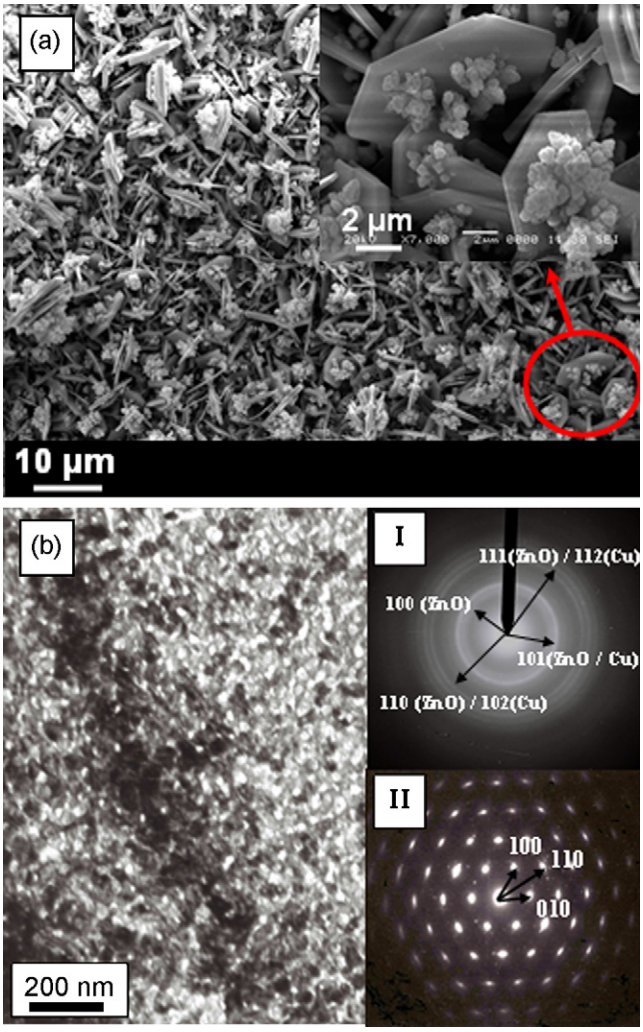

Fig. 2. (a) Low and high magnified SEM images and (b) TEM micrograph of the Cu/ZnO nanocomposite film. The inset of TEM micrograph shows two distinct SAED patterns corresponding to the Cu nanoparticles and ZnO sheets (b(I)) and ZnO microsheets (b(II)).

results. The selected area electron diffraction (SAED) patterns were performed from different areas on the TEM grid. During the TEM analysis in the electron diffraction mode, we have observed two distinct diffraction images, shown as inset of Fig. 2(b). The SEAD pattern in Fig. 2b(I) consisting of a set of concentric rings, indicative of the 'polycrystalline' nature, which originate from the copper nanoparticles and ZnO sheets. The SAED pattern in Fig. 2b(II), comprises of well resolved spots depicting 6 fold symmetry (hexagonal) corresponding to the crystalline nature of the ZnO microsheet with [0 0 1] as the preferred growth direction. Similar SAED patterns have been reported for ZnO sheets by various groups [19,20]. The compositional analysis and purity of the as-synthesized films were obtained using EDS. A typical EDS spectrum (Fig. 3) shows the presence of Cu, Zn and O with atomic percentage of 18%, 44% and 38%, respectively.

ZnO films without Cu particles were also synthesized under the previous electrodeposition conditions without adding $CuCl_2$ in the electrolyte. In order to reveal the influence of Cu nanoparticles on the electronic properties, the PL spectra of the ZnO films, with and without Cu nanoparticles, were recorded in the spectral range 350–650 nm at room temperature and are shown in Fig. 4. Both the spectra exhibit the same spectral features except the intensity. The intensity of the characteristic peaks in the PL spectrum of Cu/ZnO nanocomposite film is observed to be smaller than that for the ZnO

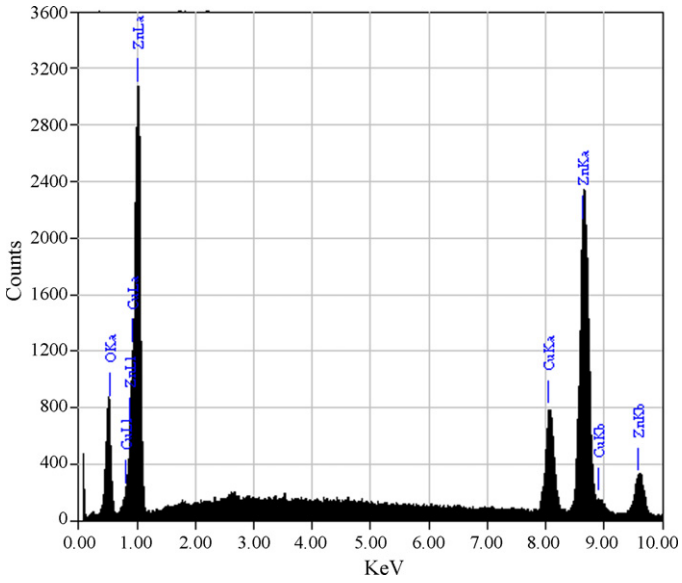

Fig. 3. EDS spectrum of the Cu/ZnO nanocomposite film.

film. The observed PL spectrum of the Cu/ZnO nanocomposite film is similar to that reported for Cu doped ZnO nanoparticles [21]. The observed decrease in the overall intensity of the PL spectrum is attributed to the decrease in the oxygen vacancies [22]. In case of ZnO nanostructures the oxygen vacancies are mainly restricted to the surface. In the present case, the presence of the Cu nanoparticles on the ZnO microsheets is expected to reduce the effective surface area of the sheets, which in turn leads to decrease in the concentration of the oxygen vacancies. Although, possibility of surface oxidation of copper (after the films are synthesized) cannot be ruled out, the oxide phases thus formed are quantitatively so small that they will not effect the XRD and/or PL spectra.

The field emission current density versus applied field (J–E) curve of the Cu/ZnO nanocomposite film recorded at the base pressure of $\sim 1 \times 10^{-8}$ mbar is depicted in Fig. 5. Before recording the I–V data, pre-conditioning in terms of removal of surface asperities and/or contaminants by residual gas ion bombardment was carried out. For this, the emitter was kept at −2 kV with respect to the anode for 5 min duration. From the J–E curve the value of the turn-on field, required to draw the emission current density of 0.1 μA/cm^2, is observed to be ~1.56 V/μm. As the applied voltage was increased, the emission current was observed to increase rapidly and a current density of ~100 μA/cm^2 has been drawn at the applied field of

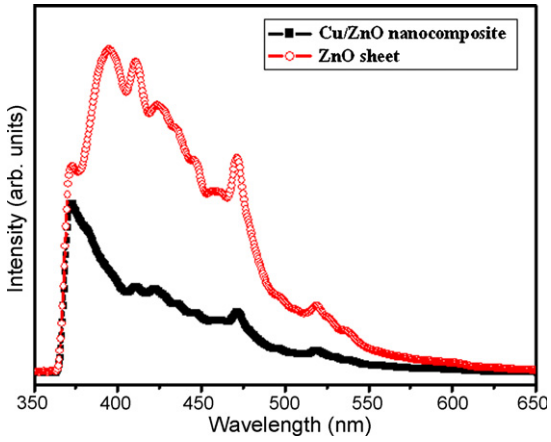

Fig. 4. Photoluminescence spectra of the ZnO and Cu/ZnO nanocomposite films.

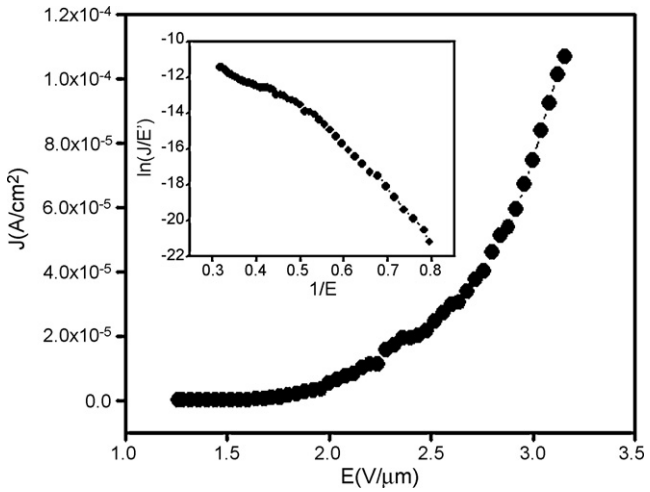

Fig. 5. Field emission current density versus applied field (J–E) curve of the Cu/ZnO nanocomposite film. The inset depicts the corresponding Fowler–Nordheim (F–N) plot.

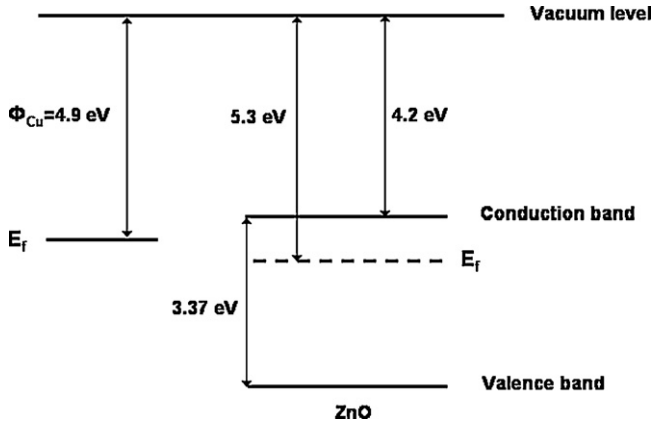

Fig. 6. Schematic of the energy band diagrams of copper and ZnO.

$\sim$3.12 V/μm. In the present study, the current density J is defined as $J = I/A$, where I is the measured value of emission current and A is the overall area of the emitter (1 cm^2). The applied field (E) is defined as $E = V/d$, where V is the applied potential and d is the separation between the anode and the cathode. This field is also referred to as an average field.

In order to compare the present results, data of the applied field values and the corresponding current densities for various ZnO, CuO and Cu nanostructures is depicted in Table 1. It is clearly seen from the table that the Cu/ZnO nanocomposite film has lower value of the applied field, corresponding to both low and very high current densities, as compared to the other nanostructures. The superior emission behaviour exhibited by the Cu/ZnO nanocomposite film emitter can be attributed to the existence of Cu nanoparticles. We have measured sheet resistances of the ZnO film synthesized without addition of $CuCl_2$ in the electrolyte and Cu/ZnO nanocomposite film using two probe method, which are found to be $\sim$166 Ω and $\sim$12 Ω, respectively. The Cu nanoparticles present on the surface of the ZnO microsheets form a heterojunction (metal–semiconductor) and donate electrons to ZnO readily, thereby increasing the electrical conductivity with decrease in the oxygen vacancies of the nanocomposite film. The enhanced field emission behaviour of the Cu/ZnO nanocomposite film can be analyzed considering the energy band diagram, schematically depicted in Fig. 6. The work function of copper (4.9 eV) [24] being smaller than that of ZnO (5.3 eV) enables transfer of electrons from copper nanoparticles to ZnO, as reflected in the increased electrical conductivity of the nanocomposite film. This is also supported by the electron affinities of copper and ZnO, which are 1.235 eV and 2.087 eV, respectively. In addition, the 'local' electric field at the most protruding Cu nanoparticles leads to electron emission from such particles, thereby increasing the number of emission sites. Thus the superior field emission behaviour of the Cu/ZnO nanocomposite film emitter can be attributed to the combined effect of (i) enhanced electrical conductivity of the film due to electron transfer from Cu particles to ZnO and (ii) increase in the number of emission sites envisaged by the smaller size of the protruding Cu nanoparticles.

The inset of Fig. 5 depicts the corresponding $\ln(J/E^2)$ versus $(1/E)$ curve, the Fowler–Nordheim (F–N) [23] plot, derived from the observed I–V characteristic. The F–N plot exhibits nonlinear behaviour over the entire range of the applied field, indicating the semiconducting nature of the emitter. Similar nonlinear F–N plots have been reported for ZnO and other semiconductors [25–27].

Along with the emission characteristics, the field emission current stability is one of the important parameters in the context of practical applications of the cold cathodes. The emission current stability has been investigated at the pre-set current value of 10 μA at the pressure of $\sim 1.0 \times 10^{-8}$ mbar. Fig. 7 depicts the emission current versus time (I–t) plot recorded over a duration of more than 5 h. The emission current stability is observed to be good with fluctuations within ±10% of the average value. The current fluctuations may be due to adsorption, desorption of the

Table 1
Key performance parameters of the various field emitters (nanostructures/thin film). The turn-on field and threshold field refer to the values of applied field required to draw emission current density of $\sim$0.1 μA/cm^2 and 1 mA/cm^2, respectively.

Material	Morphology	Synthesis method	Turn-on field (V/μm)	Threshold field (V/μm)	References
ZnO	Nanosheets	Electrochemical deposition	9.5 for 10 μA/cm^2	–	[6]
	Nanowalls	Electrochemical deposition	3.6	6.6 (0.34 mA/cm^2)	[7]
	Nanoneedles	Chemical route	2.3	3.85 (1 μA/cm^2)	[8]
	Nanopins	Vapour transport process	1.92	5.9	[9]
	Nanowires	Vapour phase growth	6	11.0	[10]
	Nanorods	Thermal evaporation process	4.1	7.5	[11]
	Nanotubes	Hydrothermal reaction	7	17.8	[12]
Cu	Nanowires	Electrochemical deposition	18 for 20 μA/cm^2	25.0 (0.4 mA/cm^2)	[13]
CuO	Nanowires	Chemical route	3.6	–	[14]
	Nanowires	Vapour solid process	3.5–4.5 for 10 μA/cm^2	7.0 (450 μA/cm^2)	[15]
	Nanobelts	Aqueous reaction	–	11 (10 μA/cm^2)	[16]
Cu/ZnO	Nanoparticles on 2 D hexagonal sheets	Electrochemical deposition	1.56	3.12 (0.1 mA/cm^2)	Present study

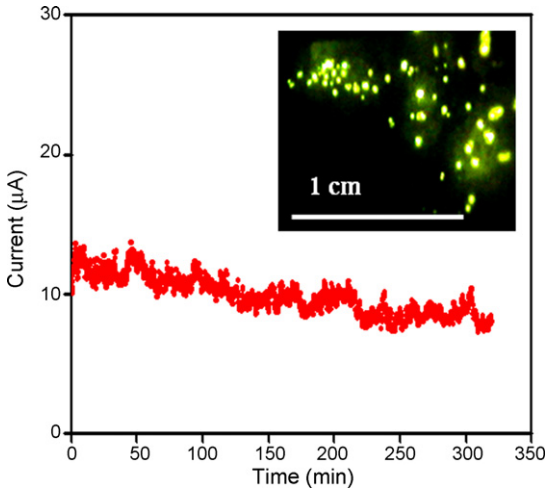

Fig. 7. Field emission current stability (*I*–*t*) plot of the Cu/ZnO nanocomposite film. The inset shows a typical field emission image.

residual gas atoms/molecules on the emitter surface. An interesting feature of the Cu/ZnO nanocomposite emitter is that the average emission current remains fairly constant over the entire duration and shows no signs of degradation of the emitter.

The post-field emission SEM studies of Cu/ZnO nanocomposites were carried out in order to see the structural stability of the film. It is interesting to note that the SEM images showed no significant changes in the emitter surface morphology. The inset of Fig. 7 shows a typical field emission micrograph. The temporal changes in the image spots intensity have been observed to be commensurate with the emission current fluctuation as seen in the *I*–*t* plot. The size and shape of the image spots indicate that the emission mainly originate from the copper nanoparticles.

4. Conclusions

Cu/ZnO nanocomposite films have been synthesized by cathodic electrodeposition on Zn substrate. The XRD pattern shows presence of ZnO and Cu. The SEM and TEM images reveal the formation of hexagonal two-dimensional ZnO sheets and Cu nanoparticles. The SAED images verify the nanocrystalline nature of the Cu particles. From the field emission studies, the turn-on field required for the 0.1 $\mu A/cm^2$ is found to be 1.56 V/μm, which is better than the values reported for other ZnO nanostructures. The Cu/ZnO nanocomposite film shows good emission current stability at the present value of 10 μA over the duration of more than 5 h. The simplicity of the synthesis route coupled with the promising field emission properties makes the electrochemically synthesized Cu/ZnO nanocomposite film suitable for high current density field emission applications.

Acknowledgements

F. Jamali Sheini would like to thank Islamic Azad University, Ahwaz Branch, Iran, for the award of Research Fellowship. The field emission studies were carried out under CNQS (Center for Nanoscience and Quantum System), University of Pune.

References

[1] S.H. Jo, D. Banerjee, Z.F. Ren, Appl. Phys. Lett. 85 (2004) 1407.
[2] L. Liao, J.C. Li, D.F. Wang, C. Liu, C.S. Liu, Q. Fu, L.X. Fan, Nanotechnology 16 (2005) 985.
[3] J.M. Lin, H.Y. Lin, C.L. Cheng, Y.F. Chen, Nanotechnology 17 (2006) 4391.
[4] C. Ye, Y. Bando, X. Fang, G. Shen, D. Golberg, J. Phys. Chem. C 111 (2007) 12673.
[5] S.K. Marathe, P.M. Koinkar, S.S. Ashtaputre, V. Sathe, M.A. More, S.K. Kulkarni, Thin Solid Films, in press.
[6] B. Cao, X. Teng, S.H. Heo, Y. Li, S.O. Cho, G. Li, W. Cai, J. Phys. Chem. C 111 (2007) 2470.
[7] D. Pradhan, M. Kumar, Y. Ando, K.T. Leung, Nanotechnology 19 (2008) 35603.
[8] S.K. Marathe, P.M. Koinkar, S.S. Ashtaputre, M.A. More, S.W. Gosavi, D.S. Joag, S.K. Kulkarni, Nanotechnology 17 (2006) 1932.
[9] C.X. Xu, X.W. Sun, Appl. Phys. Lett. 83 (2003) 3806.
[10] C.J. Lee, T.J. Lee, S.C. Lyu, Y. Zhang, H. Ruh, H.J. Lee, Appl. Phys. Lett. 81 (2002) 3648.
[11] Q. Zhao, X.Y. Xu, X.F. Song, X.Z. Zhang, D.P. Yu, C.P. Li, L. Guo, Appl. Phys. Lett. 88 (2006) 033102.
[12] A. Wei, X.W. Sun, C.X. Xu, Z.L. Dong, M.B. Yu, W. Huang, Appl. Phys. Lett. 88 (2006) 213102.
[13] S. Xavier, S. Matefi-Tempfli, E. Ferain, S. Purcell, S. Enouz-Vedrenne, L. Gangloff, E. Minoux, L. Hudanski, P. Vincent, J.-P. Schnell, D. Pribat, L. Piraux, P. Legagneux, Nanotechnology 19 (2008) 215601.
[14] W.-Y. Sung, W.-J. Kim, S.-M. Lee, H.-Y. Lee, Y.-H. Kim, K.-H. Park, S. Lee, Vacuum 81 (2007) 851.
[15] Y.W. Zhu, T. Yu, F.C. Cheong, X.J. Xu, C.T. Lim, V.B.C. Tan, J.T.L. Thong, C.H. Sow, Nanotechnology 16 (2005) 88.
[16] J. Chen, S.Z. Deng, N.S. Xu, W. Zhang, X. Wen, S. Yang, Appl. Phys. Lett. 83 (2003) 746.
[17] N.S. Ramgir, D.J. Late, A.B. Bhise, I.S. Mulla, M.A. More, D.S. Joag, V.K. Pillai, Nanotechnology 17 (2006) 2730.
[18] F. Jamali Sheini, I.S. Mulla, D.S. Joag, M.A. More, Thin Solid Films (2009), doi:10.1016/j.tsf.2009.04.046.
[19] S.-K. Min, R.S. Mane, O.-S. Joo, T. Ganesh, B.W. Cho, S.-H. Han, Curr. Appl. Phys. 9 (2009) 492.
[20] C.X. Xu, G.P. Zhu, J. Kasim, S.T. Tan, Y. Yang, X. Li, Z.X. Shen, X.W. Sun, Curr. Appl. Phys. 9 (2009) 573.
[21] K. Borgohain, S. Mahamuni, Semicond. Sci. Technol. 13 (1998) 1154.
[22] H. Yang, Y. Xiao, K. Liu, Q. Feng, J. Am. Ceram. Soc. 91 (2008) 1591.
[23] R.H. Fowler, L.W. Nordheim, Proc. R. Soc. London: Ser. A 119 (1928) 173.
[24] D.R. Lide (Ed.), CRC Handbook of Chemistry and Physics, 85th ed., CRC Press, Boca Raton, FL, 2005.
[25] F. Jamali Sheini, D.S. Joag, M.A. More, Ultramicroscopy 109 (2009) 418.
[26] A.A. Al-Tabbakh, M.A. More, D.S. Joag, N.S. Ramgir, I.S. Mulla, V.K. Pillai, Appl. Phys. Lett. 90 (2007) 162102.
[27] A.B. Bhise, D.J. Late, N.S. Ramgir, M.A. More, I.S. Mulla, V.K. Pillai, D.S. Joag, Appl. Surf. Sci. 253 (2007) 9159.